Experimental demonstration of spectral sideband splitting in strongly dispersion oscillating fibers

Fang Feng, Philippe Morin, Yanne Kouomou Chembo, Alexej Sysoliatin, Stefan Wabnitz, Christophe Finot

Experimental demonstration of spectral sideband splitting in strongly dispersion oscillating fibers

Fang Feng [1], Philippe Morin [1], Yanne K. Chembo [2], Alexej Sysoliatin [3], Stefan Wabnitz [4] and Christophe Finot [1,*]

[1] *Laboratoire Interdisciplinaire Carnot de Bourgogne, UMR 6303, 9 av. Alain Savary, 21078 Dijon, France*
[2] F *EMTO-ST/Optics department, UMR 6174, 15B Avenue des Montboucons, 25030 Besançon, France*
[3] *Fiber Optics Research Center, 11933 Moscow, Russia*
[4] *Dipartimento di Ingegneria dell'Informazione, Università degli Studi di Brescia, via Branze 38, 25123, Brescia, Italy*
**Corresponding author: christophe.finot@u-bourgogne.fr*

Received Month X, XXXX; revised Month X, XXXX; accepted Month X, XXXX; posted Month X, XXXX (Doc. ID XXXXX); published Month X, XXXX

By using a highly nonlinear, dispersion oscillating optical fiber operating in the telecom C band, we experimentally demonstrate the splitting experienced by quasi-phase matched gain sidebands in the strongly dispersion managed regime of a dispersion oscillating fiber as the power of a continuous-wave pump laser is increased over a certain threshold value. Excellent agreement is found between the theoretical predictions and our experimental measurements.

OCIS Codes: (060.4370) Nonlinear optics, fibers, (190.4380) Nonlinear optics, four-wave mixing, (190.4410) Nonlinear optics, parametric process
http://dx.doi/org/XXXXXX

Modulation instability (MI) is an ubiquitous nonlinear process that has been widely investigated in various fields of physics and applications including plasmas, hydrodynamics and optics, to cite a few. In the presence of a high power continuous wave (CW), MI leads to the emergence and amplification of gain sidebands in the wave spectrum. In nonlinear fiber optics, such a process has been demonstrated in fibers with anomalous, constant group velocity dispersion (GVD) [1], as well as in normal GVD fibers by enabling the fulfillment of the nonlinear phase-matching condition through either fourth-order dispersion [2], birefringence or a multimodal structure [3, 4]. More recently, a renewed experimental and theoretical interest in MI studies has been stimulated by the availability of fibers with a longitudinal and periodic modulation of their dispersion properties [5]. Indeed, thanks to the periodic dispersion landscape, which leads to quasi-phase-matching (QPM) of the nonlinear four-wave mixing (FWM) process, MI sidebands can be observed even in the regime of normal average GVD of a dispersion-oscillating optical fiber (DOF) [6-8]. Recent experimental studies have indeed confirmed the QPM-induced MI process in the normal GVD regime of a microstructure DOF around 1 μm [5], as well as of conventional highly nonlinear DOF at telecom wavelengths [9, 10].

MI induced by the longitudinal variations of chromatic dispersion has been theoretically investigated earlier for a wide range of configurations, ranging from fibers with a sinusoidal dispersion profile and a spatial period of a few tens of meters [5, 9], up to dispersion-managed optical transmission fiber spans with periods of several kilometers [6, 11, 12]. Whenever the dispersion fluctuations can be considered as a perturbation to nonlinear wave propagation, that is when their amplitude is smaller or comparable with the value of the average dispersion, QPM-induced MI leads to the emergence of well-separated, and unequally spaced gain sidebands, symmetrically placed around the pump. On the other hand, it has been recently theoretically shown that when the amplitude of dispersion fluctuation grows much larger than the average GVD (strong dispersion management regime), a spectral splitting process may occur in the sideband spectrum [13].

In this letter we report the first experimental validation of this prediction, by using a highly nonlinear DOF pumped in the telecom C band. As a basis for our discussion, let us first recall the expected evolution of QPM sidebands as the pump power is increased. For that purpose, we consider a continuous wave (CW) pump and make use of both a Floquet linear stability analysis (LSA) as well as of the existing analytical laws. Next, we will describe the implemented experimental setup and the corresponding experimental results which demonstrate the transition from the regime of usual QPM-induced MI to the novel regime of MI which exhibits spectral sideband splitting. Finally, we compare our experimental results with the full numerical simulations of the nonlinear Schrödinger equation (NLSE).

The evolution of the optical field in an optical fiber can be described by the NLSE :

$$i\frac{\partial \psi}{\partial z} - \frac{\beta_2(z)}{2}\frac{\partial^2 \psi}{\partial t^2} + \gamma |\psi|^2 \psi = 0 \quad (1)$$

where ψ is the complex electrical field, z is the propagation distance and t the retarded time. The NLSE includes both the Kerr nonlinearity γ and the second-order dispersion β_2, which is supposed to periodically evolve in the longitudinal direction according to the sinusoidal law

$$\beta_2(z) = \beta_{2av} + \beta_{2amp} \sin(2\pi z / \Lambda) \quad (2)$$

where β_{2av} is the average dispersion of the fiber, β_{2amp} is half of the peak-to-peak amplitude of the dispersion variation, and Λ is the spatial period of the fluctuations.

In the presence of relatively weak amplitude sinusoidal longitudinal GVD variations, QPM of the FWM (or MI) process leads to the appearance of resonant gain sidebands, whose angular frequency shift relative to the pump can be analytically predicted as follows [6] :

$$\Omega_p = \pm\sqrt{\frac{2\pi p / \Lambda - 2\gamma P}{\beta_{2av}}} \quad (3)$$

with $p = 1, 2, 3 \ldots$ More recently, it has been shown that the gain g_p experienced by the p^{th} sidebands may also be analytically predicted by the formula [14] :

$$g_p = 2\gamma P \left| J_p\left(\frac{\beta_{2amp}\,\Omega_p^2}{2\pi / \Lambda}\right)\right| \quad (4)$$

where J_p is the Bessel function of order p.

In order to illustrate the process of spectral splitting, we consider here the same optical fiber that was previously employed in refs. [9, 10]. This 400-m long highly nonlinear fiber has a nonlinear coefficient of 10 $W^{-1}km^{-1}$. The amplitude of dispersion fluctuations β_{2amp} is estimated to be 2 ps^2/km, with a spatial period Λ=20 m. By changing the pumping wavelength, it is possible to access different values of the average dispersion β_{2av}. Therefore, we have compared spectra which are obtained for the pumping wavelengths of 1536 and 1554 nm. The corresponding average dispersion values β_{2av} are 0.7 ps^2/km and 0.13 ps^2/km, respectively, so that the ratio $\beta_{2amp} / \beta_{2av}$ is equal to 2.8 and 15.4 in the two cases. Let us consider the resulting MI gain spectra for a CW pump power ranging in the interval between 0 and 11 W.

Equations (3) and (4) do provide accurate predictions of the value of the sideband gain which is expected at the resonant frequencies Ω_p. However these equations do not give us an insight on the actual shape of the gain sideband around those frequencies. Using the LSA of the CW pump by means of the Floquet's approach has been shown to be a very powerful method to calculate the details of MI gain sidebands for optical fibers with spatially periodic parameters [13, 15, 16]. In particular the Floquet LSA enables to correctly describe the spectral sideband splitting effect.

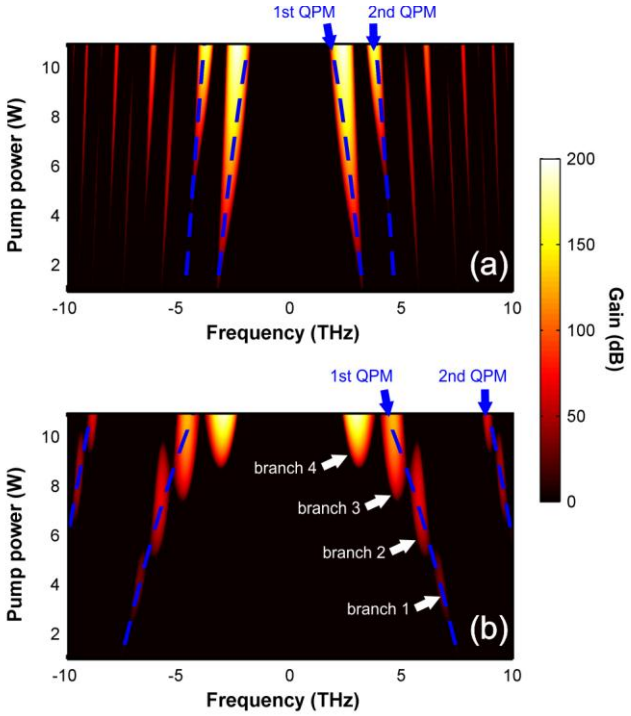

Fig. 1. Evolution of the output gain spectrum according to the input power for an average dispersion of 0.7 ps^2/km (a) and 0.13 ps^2/km (b). The corresponding pumping wavelengths are 1536 and 1554 nm. Results are obtained from the linear stability analysis based on the Floquet theory. The predictions from Eq. (3) are plotted with blue line.

Therefore we may take advantage of this method to plot the theoretically expected gain sideband for the two previously mentioned pumping wavelengths. The corresponding results, showing the impact of the pump power on the MI gain spectrum, are summarized in Fig. 1. For the pump wavelength of 1536 nm (panel a), the two main sidebands are provided by the 1st and 2nd QPM conditions. They experience a continuous growth and their position is in excellent agreement with Eq. (3).

The behavior of the MI spectrum is radically different for a high ratios β_{2amp}/β_{2av}>>1, as illustrated by panel b of Fig.1. Indeed, in this configuration the MI gain which is predicted by Eq. (4) exhibits a non-monotonic evolution with pump power. More importantly, for some values of pump power the gain g_p vanishes. Consequently, several branches of the 1st QPM sideband can be distinguished (four in our case, with frequency offsets around 6.8, 5.8, 4.7 and 3 THz, respectively) in panel b of Fig.1: hence the spectral splitting phenomenon is observed. By comparing panels a and b of Fig.1 we may note that the observation of relatively sideband gains (i.e., above 150 dBs) requires higher pump power values in the strongly dispersion oscillating regime.

Our experimental setup for the observation of MI sideband splitting is depicted on Fig. 2(a). A CW pump delivered by a wavelength tunable external cavity laser is phase modulated at a low frequency (typically 100 MHz), in order to avoid any detrimental Brillouin backscattering upon propagation in the fiber. Next an intensity modulator is used to temporally slice into the CW pump.

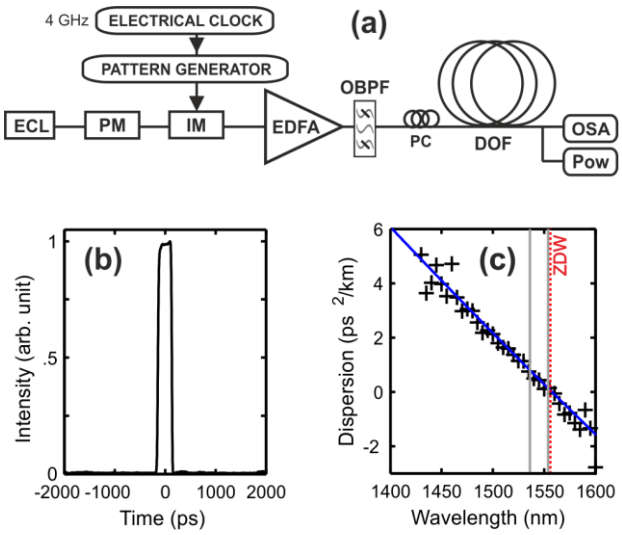

Fig.2. (a) Experimental setup. Details of the pump pulse (b) and of the fiber dispersive properties (c).

This modulator is driven by a deterministic non-return-to-zero sequence of a single one followed by 31 zeros repeating at a frequency of 4 GHz. This enables to achieve, for a given average power, a more than twenty-fold increase of the peak power of the resulting long pulse. The resulting pulses repeat every 8 ns, have a 250 ps duration and an intensity profile close to a super-Gaussian shape as outlined on Fig. 2(b). A high power erbium-doped fiber amplifier (EDFA) is then used to obtain an average power up to 33 dBm. A narrow optical bandpass filter (OBPF) is inserted to limit the build-up of amplified spontaneous emission (ASE), and to adjust the power level at the DOF input.

The highly nonlinear DOF under test was designed and fabricated to have a zero dispersion wavelength (ZDW) in the telecom C band (ZDW = 1556 nm). The fiber preform was prepared by the MCVD process using mixtures of $GeCl_4$, $SiCl_4$ and SiF_4 in order to obtain the necessary refractive index profile. Fig. 2(c) shows the measured values of the average dispersion of the fiber as a function of wavelength. The values estimated at wavelengths 1536 and 1554 nm corresponds to the values used in the previous numerical simulations. At the output of the fiber, a 90/10 coupler is used to simultaneously monitor the output spectrum on an optical spectrum analyzer (OSA) and the output power on a power meter (Pow).

Let us first consider the MI which is induced by a pump centered at 1536 nm. The corresponding results are plotted on Fig. 3(a) for two different power levels. For a power of 3.5 W, we clearly observe the emergence of the 1st QPM sideband (grey curve). The small side-lobe in the vicinity of the pump at lower frequencies is due to residual ASE. For relatively high pump powers (i.e., 7 W, see the black solid curve), the intensity of the 1st QPM sideband is largely increased, and its central frequency is shifted towards lower frequencies, in agreement with Eq. (3). In this case we also observe in Fig.3(a) the emergence of the 2nd QPM sideband, as well as the generation of a set of equally spaced, widely shifted sidebands that originate from the cascaded or multiple four wave mixing (MFWM) process involving the pump and the 1st QPM sideband [9].

A more systematic study of the influence of the input pump power on the output MI spectrum is presented on Fig. 4(a).

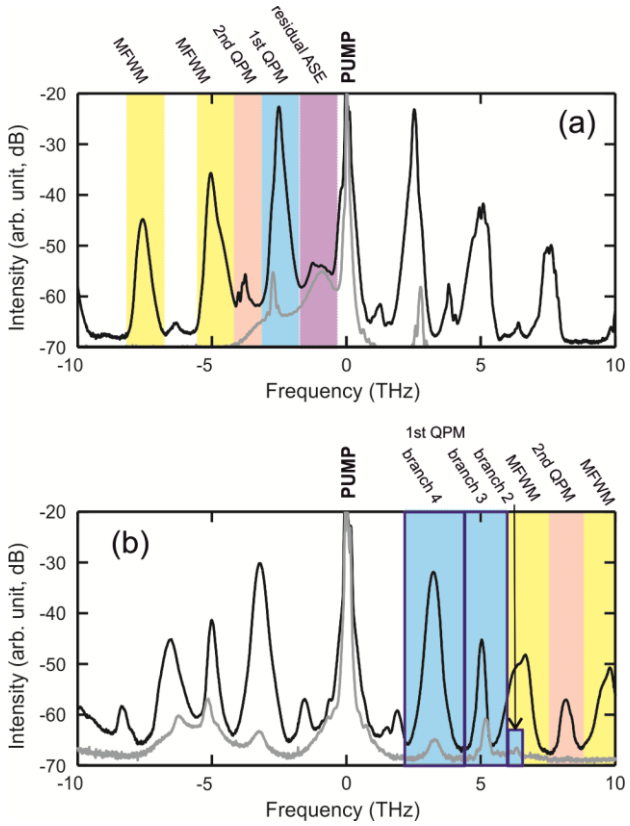

Fig. 3. (a) Experimental output spectrum for pump wavelength of 1536 nm for pump powers of 3.5 and 7 W (grey and solid black lines respectively). (b) Experimental output spectrum for pump wavelength of 1554 nm for pump powers of 7 and 9 W (grey and solid black lines respectively).

The experimental results obtained by the averaging of 36 measurements confirm the generation and growth of the 1st and 2nd QPM sidebands. Their evolution as a function of pump power is in qualitative agreement with the Floquet LSA results presented Fig. 1(a), except for the emergence of MFWM sidebands. For pump powers higher than 10 W, the different sidebands merge and a continuum is formed, with a noticeable spectral asymmetry owing to the Raman effect The overall spectral behavior is consistent with our previous measurements carried out with a ns Q-switched laser emitting at 1534 nm [9].

The picture is very different when dealing with a pump whose wavelength is located in the vicinity of the ZDW (see Fig. 3(b)), hence a more careful analysis is required in this case. In agreement with the theoretical prediction of Fig.1, higher pump powers are required to reach a level that can be detected on the OSA. The results obtained for a pump power of 7W reveal the emergence of three distinct sidebands, which result from the splitting of the 1st QPM sideband. The most powerful branch 3 is shifted by 5 THz from the pump. When increasing the pump power to 9 W, the branch 4 which is shifted by nearly 3 THz grows the largest, in agreement with the Floquet analysis. Once again, FWM-induced sidebands are also observed and they overlap branch 2 (shifted by 6 THz) of the 1st QPM sideband.
The experimental signature of MI sideband splitting was clearly confirmed by systematic measurements of the MI spectrum evolution (24 measurements are summarized on Fig. 4(b)).

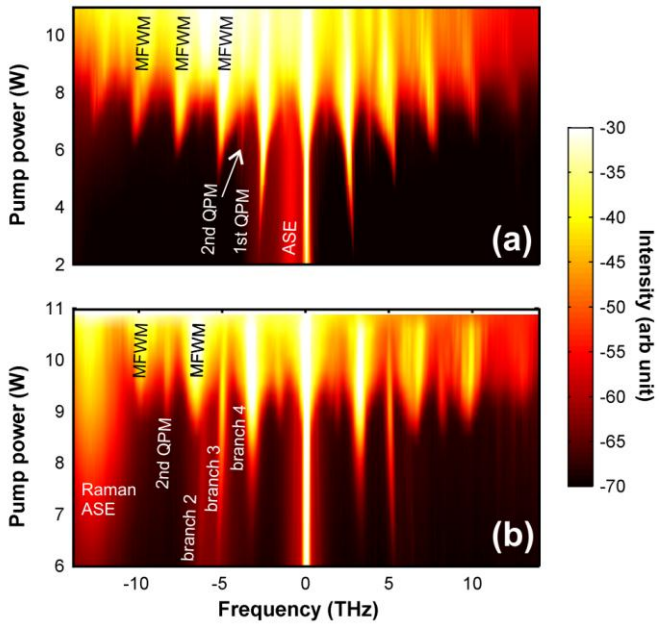

Fig. 4. Evolution of the output spectrum according to the input power recorded experimentally for a pump wavelength of (a) 1536 nm and (b) 1554 nm. Results are plotted using a 40 dB dynamics.

Here the emergence and growth of the 2nd QPM sideband is also be observed, along with a broad Raman peak at -13 THz. For pump powers higher than 10 W, a continuum is formed.

In order to further validate our experimental results as well as the analysis of the sideband splitting process, we carried out simulations of the propagation of the pulsed pump in the DOF.

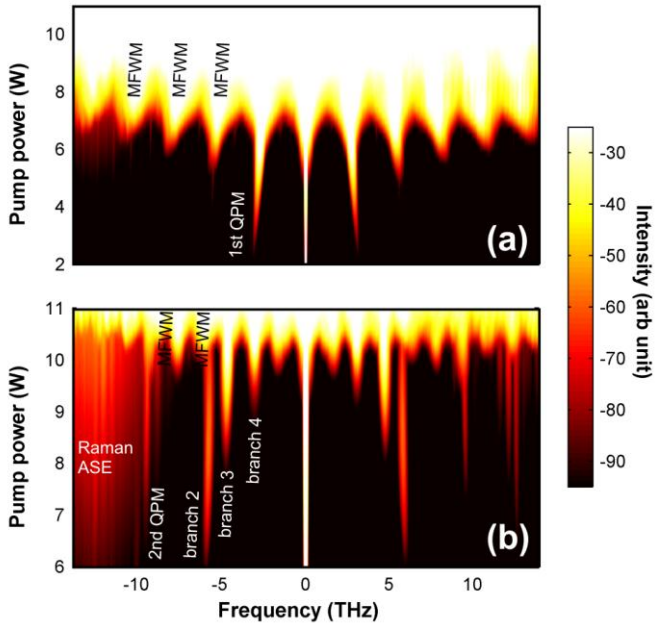

Fig. 5. Evolution of the output spectrum according to the power for a pump wavelength of (a) 1536 nm and (b) 1554 nm.. Results obtained from the numerical integration of the extended NLSE. Results are averaged over 36 simulations.

For this purpose, we used the extended NLSE including the third order dispersion term (4.7 10^{-5} ps^3/m) and the delayed Raman response of silica. Given their potential impact in the process of spectral splitting, we also included linear fiber loss (0.7 dB/km) [13] and the pump pulse shape [17]. Simulation results are summarized in Fig. 5, and reproduce nearly all of experimentally observed features which were not predicted by the LSA of Fig. 1.

In conclusion, we presented the first experimental demonstration of the sideband spectral splitting effect in strongly dispersion oscillating fibers. The Floquet-based LSA was completed by pulse propagation simulations.

We thank Julien Fatome and Kamal Hammani for stimulating discussions. We acknowledge financial support of the Conseil Regional de Bourgogne (Pari Photcom), funding of the Labex ACTION program (ANR-11-LABX-01-01), the Italian Ministry of University and Research (grant no. 2012BFNWZ2), the Landau Network-Cariplo Foundation and the Russian Science Foundation (RSCF 14-12-01338).

References

1. K. Tai, A. Hasegawa, and A. Tomita, Phys. Rev. Lett. **56**, 135-138 (1986).
2. S. Pitois and G. Millot, Opt. Commun. **226**, 415-422 (2003).
3. G. Millot and S. Wabnitz, J. Opt. Soc. Am. B **31**, 2754-2768 (2014).
4. G. Millot, S. Pitois, P. Tchofo-Dinda, and M. Haelterman, Opt. Lett. **22**, 1686-1688 (1997).
5. M. Droques, A. Kudlinski, G. Bouwmans, G. Martinelli, and A. Mussot, Opt. Lett. **37**, 4832-4834 (2012).
6. N. J. Smith and N. J. Doran, Opt. Lett. **21**, 570 (1996).
7. F. K. Abdullaev, S. A. Darmanyan, A. Kobyakov, and F. Lederer, Phys. Lett. A **220**, 213-218 (1996).
8. A. Armaroli and F. Biancalana, Opt. Express **20**, 25096-25110 (2012).
9. C. Finot, J. Fatome, A. Sysoliatin, A. Kosolapov, and S. Wabnitz, Opt. Lett. **38**, 5361-5364 (2013).
10. F. Feng, J. Fatome, A. Sysoliatin, Y. K. Chembo, S. Wabnitz, and C. Finot, Electron. Lett. **50**, 168-170 (2014).
11. F. Consolandi, C. De Angelis, A.-D. Capobianco, G. Nalesso, and A. Tonello, Optics Communications **208**, 309-320 (2002).
12. S. Ambomo, C. M. Ngabireng, P. T. Dinda, A. Labruyère, K. Porsezian, and B. Kalithasan, Journal of the Optical Society of America B **25**, 425-433 (2008).
13. C. Finot, F. Feng, Y. K. Chembo, and S. Wabnitz, Opt. Fiber. Technol. **20**, 513-519 (2014).
14. M. Droques, A. Kudlinski, G. Bouwmans, G. Martinelli, and A. Mussot, Phys. Rev. A **87**, 013813 (2013).
15. A. Armaroli and F. Biancalana, Opt. Lett. **39**, 4804-4807 (2014).
16. M. Conforti, A. Mussot, A. Kudlinski, and S. Trillo, Opt. Lett. **39**, 4200-4203 (2014).
17. C. Finot and S. Wabnitz, in preparation (2014).

References

1. K. Tai, A. Hasegawa, and A. Tomita, "Observation of modulational instability in optical fibers," Phys. Rev. Lett. **56**, 135-138 (1986).
2. S. Pitois and G. Millot, "Experimental observation of a new modulational instability spectral window induced by fourth-order dispersion in a normally dispersive single-mode optical fiber," Opt. Commun. **226**, 415-422 (2003).
3. G. Millot and S. Wabnitz, "Mini-Review of Nonlinear Polarization Effects in Optical Fibers: Polarization Attraction and Modulation Instability," J. Opt. Soc. Am. B **31**, 2754-2768 (2014).
4. G. Millot, S. Pitois, P. Tchofo-Dinda, and M. Haelterman, "Observation of modulational instability induced by velocity-matched cross-phase modulation in a normally dispersive bimodal fiber," Opt. Lett. **22**, 1686-1688 (1997).
5. M. Droques, A. Kudlinski, G. Bouwmans, G. Martinelli, and A. Mussot, "Experimental demonstration of modulation instability in an optical fiber with a periodic dispersion landscape," Opt. Lett. **37**, 4832-4834 (2012).
6. N. J. Smith and N. J. Doran, "Modulational instabilities in fibers with periodic dispersion management," Opt. Lett. **21**, 570 (1996).
7. F. K. Abdullaev, S. A. Darmanyan, A. Kobyakov, and F. Lederer, "Modulational instability in optical fibers with variable dispersion," Phys. Lett. A **220**, 213-218 (1996).
8. A. Armaroli and F. Biancalana, "Tunable modulational instability sidebands via parametric resonance in periodically tapered optical fibers," Opt. Express **20**, 25096-25110 (2012).
9. C. Finot, J. Fatome, A. Sysoliatin, A. Kosolapov, and S. Wabnitz, "Competing four-wave mixing processes in dispersion oscillating telecom fiber," Opt. Lett. **38**, 5361-5364 (2013).
10. F. Feng, J. Fatome, A. Sysoliatin, Y. K. Chembo, S. Wabnitz, and C. Finot, "Wavelength conversion and temporal compression of a pulse train using a dispersion oscillating fibre," Electron. Lett. **50**, 168-170 (2014).
11. F. Consolandi, C. De Angelis, A.-D. Capobianco, G. Nalesso, and A. Tonello, "Parametric gain in fiber systems with periodic dispersion management," Optics Communications **208**, 309-320 (2002).
12. S. Ambomo, C. M. Ngabireng, P. T. Dinda, A. Labruyère, K. Porsezian, and B. Kalithasan, "Critical behavior with dramatic enhancement of modulational instability gain in fiber systems with periodic variation dispersion," Journal of the Optical Society of America B **25**, 425-433 (2008).
13. C. Finot, F. Feng, Y. K. Chembo, and S. Wabnitz, "Gain sideband splitting in dispersion oscillating fibers," Opt. Fiber. Technol. **20**, 513-519 (2014).
14. M. Droques, A. Kudlinski, G. Bouwmans, G. Martinelli, and A. Mussot, "Dynamics of the modulation instability spectrum in optical fibers with oscillating dispersion," Phys. Rev. A **87**, 013813 (2013).
15. A. Armaroli and F. Biancalana, "Suppression and splitting of modulational instability sidebands in periodically tapered optical fibers because of fourth-order dispersion," Opt. Lett. **39**, 4804-4807 (2014).
16. M. Conforti, A. Mussot, A. Kudlinski, and S. Trillo, "Modulational instability in dispersion oscillating fiber ring cavities," Opt. Lett. **39**, 4200-4203 (2014).
17. C. Finot and S. Wabnitz, "On the influence of the pump shape on the modulation instability process induced in a dispersion oscillating fiber.," in preparation (2014).